JOURNAL OF GUIDANCE, CONTROL, AND DYNAMICS
Vol. 22, No. 3, May–June 1999

Spacecraft Vibration Reduction Using Pulse-Width Pulse-Frequency Modulated Input Shaper

Gangbing Song
University of Akron, Akron, Ohio 44325-3903
and
Nick V. Buck and Brij N. Agrawal
Naval Postgraduate School, Monterey, California 93943

Minimizing vibrations of a flexible spacecraft actuated by on-off thrusters is a challenging task. This paper presents the first study of pulse-width pulse-frequency modulated thruster control using command input shaping. Input shaping is a technique that uses a shaped command to ensure zero residual vibration of a flexible structure. Pulse-width pulse-frequency modulation is a control method that provides pseudolinear operation for an on-off thruster. The proposed method takes full advantage of the pseudolinear property of a pulse-width pulse-frequency modulator and integrates it with a command shaper to minimize the vibration of a flexible spacecraft induced by on-off thruster firing. Compared to other methods, this new approach has numerous advantages: 1) effectiveness in vibration suppression, 2) dependence only on modal frequency and damping, 3) robustness to variations in modal frequency and damping, and 4) easy computation. Numerical simulations performed on an eight-mode model of the Flexible Spacecraft Simulator in the Spacecraft Research and Design Center at the U.S. Naval Postgraduate School demonstrate the efficacy and robustness of the method.

I. Introduction

MOST modern spacecraft attitude control systems employ on-off thrusters. On-off thrusters produce discontinuous and nonlinear control actions. These control actions may excite flexible modes of modern spacecraft, which use large, complex, and lightweight structures such as solar array panels. Designing an

Gangbing Song has been an assistant professor in the Department of Mechanical Engineering at the University of Akron since August of 1998. Prior to this position, he was an assistant research professor in the Department of Aeronautics and Astronautics for two years and a research associate in the Mechanical Engineering Department for one year, all at the Naval Postgraduate School. He received his Ph.D. in 1995 and M.S. degree in 1991, both from Columbia University. He has a U.S. patent and has published more than 40 journal and conference papers in the area of controls, robotics, vibrations, and smart structures.

LCDR Nick V. Buck, USN completed his graduate research in structures, dynamics, and control at the Naval Postgraduate School. Following completion of his thesis, he was awarded a M.S. in astronautical engineering as well as the Aeronautical and Astronautical Engineer's Degree in December 1996. In recognition of his academic standing, he received the Chief of Naval Operations Distinguished Graduate Award for space systems engineering. Prior to entering graduate school, he served as a navy test pilot, logging over 2000 flight h in 50 types of aircraft. He is currently assigned as an assistant program manager (Payload) in the National Reconnaissance Office in Washington, D.C.

Brij N. Agrawal is a professor in the Department of Aeronautics and Astronautics and Director of the Spacecraft Research and Design Center. He came to NPS in 1989 and since then has initiated a new M.S. curriculum in astronautical engineering in addition to establishing the Spacecraft Research and Design Center. He also has developed research programs in attitude control of flexible spacecraft, smart structures, and space robotics. He has written an industry recognized textbook, *Design of Geosynchronous Spacecraft*, and has a patent for an attitude pointing error correction system for geosynchronous satellites. He received his Ph.D. in mechanical engineering from Syracuse University in 1970 and his M.S. in mechanical engineering from McMaster University in 1968. He is an Associate Fellow of the AIAA.

Presented as Paper 97-3748 at the AIAA Guidance, Navigation, and Control Conference, Baltimore, MD, Aug. 7–10, 1997; received April 27, 1998; revision received Oct. 20, 1998; accepted for publication Oct. 30, 1998.

on-off thruster control system to provide fine pointing accuracy while avoiding interaction with the flexible structure poses a challenging task.

Research toward this end has been focused mainly into two areas. In one area, efficient methods to convert continuous input commands to on-off signals suitable for controlling on-off thrusters are sought. The other area focuses on modifying an existing command so that it results in less or zero residual vibration of a flexible spacecraft.

The two major approaches for thruster control are bang-bang and pulse modulation. Bang-bang control is simple in formulation, but results in excessive thruster action. Its discontinuous control actions often interact with the flexible mode of the spacecraft and result in limit cycles. Therefore, bang-bang control is not commonly used. On the other hand, pulse modulators are commonly employed due to their advantages of reduced propellant consumption and near-linear duty cycle. In general, pulse modulators produce a pulse command sequence to the thruster valves by adjusting pulse width and/or pulse frequency. Pulse modulators such as pseudorate modulator,[1] integral-pulse frequency modulator,[2,3] and pulse-width and pulse-frequency (PWPF) modulator[4–6] have been proposed. Among these, the PWPF modulator holds several superior advantages such as close to linear operation, high accuracy, and adjustable PWPF that provide scope for advanced control. This modulator was used on several spacecraft such as INTELSAT-5, INSAT, and ARABSAAT.

Notch filtering and input shaping are two commonly used methods to modify the input command to reduce vibrations of flexible structures. Between these two methods, input shaping has several superior advantages, including effectiveness in vibration cancellation, robustness to variations in modal frequency and damping ratio, and suitability for a multiple-mode system.[7] Originally, this method was designed for systems with proportional actuators. Recently, it has been extended to systems with on-off actuators.[8,9] However, existing approaches require complicated nonlinear optimization and often result in bang-bang control action.

In this paper a new approach integrating an input shaper with a PWPF modulator to provide vibration reduction for a flexible spacecraft is proposed. The control object in this paper is the Flexible Spacecraft Simulator (FSS) in the Spacecraft Research and Design Center (SRDC) at the U.S. Naval Postgraduate School. The FSS consists of a rigid circular disk representing a spacecraft's central body and an attached "L"-shape flexible appendage representing the antenna support structure. To realize this approach on the FSS, a modal analysis is first performed to identify the system modal frequency of the FSS. Next, an analysis of the PWPF modulator is conducted to recommend general parameter settings. Then, a command input shaper is designed, and the shaped command is modulated by the PWPF modulator for thruster control. Lastly, robustness analyses are carried out. This approach does not require any optimization and is easy to implement. Numerical simulations performed on an eight-mode model of the FSS demonstrate the efficacy and robustness of the method.

II. Flexible Spacecraft Simulator

The U.S. Naval Postgraduate School's FSS simulates motion about the pitch axis of a spacecraft. As shown in Fig. 1, the FSS is composed of a rigid central body and a reflector supported by an "L"-shape flexible appendage. The center body represents the main body of the spacecraft, whereas the flexible appendage represents a flexible antenna support structure. The flexible appendage is composed of a base beam cantilevered to the main body and a tip beam connected to the base beam at a right angle with a rigid elbow joint. The flexible appendage is supported by one air pad each at the elbow and tip to minimize friction.

The flexible dynamic model used in this study is derived using the hybrid-coordinate formulation.[10] The equations describing the motion of the rigid-body and the flexible appendage are

$$I_{zz}\ddot{\theta} + \sum_{i=1}^{n} D_i \ddot{q}_i = T_c + T_d \tag{1}$$

$$\ddot{q}_i + 2\zeta_i \omega_i \dot{q}_i + \omega_i^2 q_i + D_i \ddot{\theta} = 0 \tag{2}$$

Table 1 FSS cantilever and system frequencies

	Cantilever		System	
Mode	Hz	rad/s	Hz	rad/s
1	0.183	1.150	0.213	1.34
2	0.452	2.840	0.504	3.16
3	2.41	15.20	2.42	15.23
4	4.23	26.61	4.25	26.72
5	8.42	52.92	8.42	52.94
6	12.3	77.18	12.3	77.31
7	16.6	104.2	16.6	104.2
8	21.0	132.0	21.0	132.1

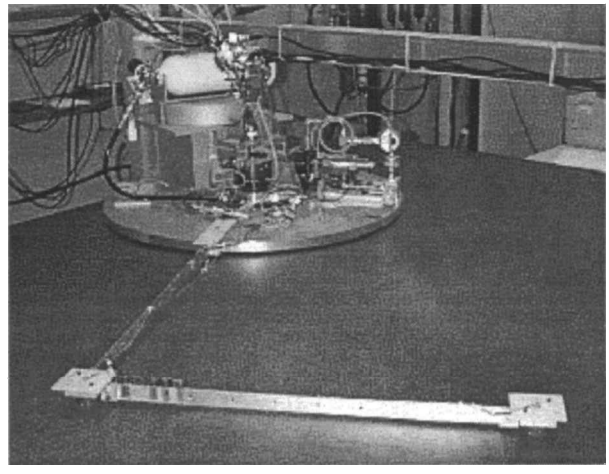

Fig. 1 FSS.

where θ is the angular position of the main body, q_i is the modal coordinate for the ith cantilever mode, I_{zz} is the moment of inertia of the system, D_i is the rigid-elastic coupling for ith mode, T_c is the control torque, T_d is the disturbance torque, ζ_i is the damping ratio of the ith mode, and ω_i is the natural frequency for the ith mode.

The rigid-elastic coupling D_i is given by

$$D_i = \int_F \left(x_F \phi_i^y - y_F \phi_i^x\right) \mathrm{d}m$$

where x_F and y_F are the coordinates of a point on the flexible structure, and ϕ_i^x and ϕ_i^y are respectively the x and y component of the ith modal vector at that point.

In discretizing the system via the finite element method, the number of modes was truncated at eight to obtain a compromise between reasonable model accuracy and computational feasibility.

The model is placed into state space in preparation for digital simulation using the MATLAB™/Simulink software package. The state-space representation of the system equations is

$$\dot{x} = Ax + Bu, \qquad y = Cx + Du$$

where the state vector x is defined as

$$x = [\theta \quad q_1 \cdots q_8 \quad \dot{\theta} \quad \dot{q}_1 \cdots \dot{q}_8]^T$$

The output y is the vector of the states; hence, C is an 18×18 identity matrix, and the feedback values of angular position and rate are measured exactly.

To find the natural frequencies of the flexible-appendage and rigid-body system, a MATLAB™ routine is used. The cantilever and system frequencies are listed in Table 1. Because low-frequency modes are generally dominant in a flexible system, in this paper the goal of design is to suppress the low-frequency-mode vibrations.

III. PWPF Modulator

The PWPF modulator produces a pulse command sequence to the thruster valves by adjusting the pulse width and pulse frequency. In its linear range the average torque produced equals the demand torque input. Compared with other methods of modulation, the

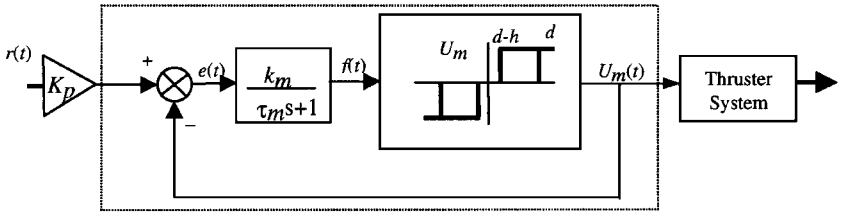

Fig. 2 PWPF modulator.

PWPF modulator has several superior advantages such as close-to-linear operation, high accuracy, and adjustable PWPF, which provide scope for advanced control.

As shown in Fig. 2, the PWPF modulator is composed of a Schmidt Trigger, a prefilter, and a feedback loop. A Schmidt Trigger is simply an on-off relay with a deadband and hysteresis. When a positive input to the Schmidt Trigger is greater than d (also denoted as E_{on}), the trigger output is U_m. Consequently, when the input falls below $d-h$ (also denoted as E_{off}), the trigger output is 0. This response is also reflected for negative inputs. The error signal $e(t)$ is the difference between the Schmidt Trigger output U_m and the system input $r(t)$. The error is fed into the prefilter whose output $f(t)$ feeds the Schmidt Trigger. The parameters of interest are the prefilter coefficients k_m and τ_m, the input gain K_p, and the Schmidt Trigger parameters d and h.

A. Modulator Static Characteristics

With a constant input the modulator has a behavior that is independent of the system in which it is used. The pulse width and period are usually fast compared with the system dynamics, and so the input to the modulator (the error signal feedback) changes slowly; the static characteristics are a good indication of how the modulator will work in most cases. Choosing appropriate parameters so that the modulator has desired static characteristics is the first step of attitude control design using the PWPF modulator.

1. On-Time and Off-Time

If the input $e(t)$ to the prefilter is a constant, e.g., e_c, then the relationship between $f(t)$ and e_c can be represented by

$$f(t) = f(0) + [k_m e_c - f(0)](1 - e^{-t/\tau_m}) \tag{3}$$

From Eq. (3) we have, as $t \to \infty$,

$$f(t \to \infty) = k_m e_c \tag{4}$$

The time taking the prefilter output to transit from d to $d-h$ is defined as the relay on-time or pulse width, denoted by T_{on} or PW. T_{on} or PW can be solved from Eq. (3) by setting $f(0) = d$, $f(T_{\text{on}}) = d-h$, and $t = T_{\text{on}}$:

$$T_{\text{on}} = PW = -\tau_m \ell_n \left\{ 1 + \frac{h}{k_m[r(t) - U_m] - d} \right\} \tag{5}$$

The off-time is defined as the time taking the prefilter output from 0 to d. According to Eq. (3), the off-time denoted by T_{off} can be solved by setting $f(0) = 0$, $f(T_{\text{off}}) = d$, and $t = T_{\text{off}}$:

$$T_{\text{off}} = -\tau_m \ell_n \left[1 - \frac{h}{k_m r(t) - (d-h)} \right] \tag{6}$$

2. Modulator Frequency

The frequency of the PWPF modulator is defined as the inverse of the period of the PWPF cycle and is given by the following equation:

$$f = \frac{1}{T_{\text{on}} + T_{\text{off}}} \tag{7}$$

3. Modulation Factor

The modulation factor of the PWPF controller is the ratio of the relay on-time to the period and is given by

$$MF = \frac{T_{\text{on}}}{T_{\text{on}} + T_{\text{off}}} \tag{8}$$

4. Conditions for Pseudolinear Operation

The maximum input $r_{\max}$ for pseudolinear operation can be solved by equating the maximum value of the prefilter output $k_m(r_{\max} - U_m)$ to the Schmidt Trigger off condition $d-h$:

$$k_m(r_{\max} - U_m) = d - h$$

i.e.,

$$\frac{k_m r_{\max} - d}{k_m U_m - h} = 1$$

or

$$r_{\max} = U_m + (d-h)/k_m \tag{9}$$

The effective deadband of the modulator is defined as the minimum input to the modulator so that $T_{\text{on}} > 0$. The $r_{\min}$ can be determined by equating the prefilter output when the Schmidt Trigger output is zero to the Schmidt Trigger on condition,

$$k_m r_{\min} = d$$

i.e.,

$$r_{\min} = d/k_m$$

It is clear that an increase of k_m reduces the size of deadband. It is reasonable to keep $k_m > 1$ to ensure that the on-threshold d is an upper bound on the deadband. With the use of the input gain K_p, the effective deadband is

$$r_{\min} = d/(k_m K_p)$$

The net effect of input gain K_p is altering the deadband by scaling the input signal. When an input signal has a large amplitude and does not fall inside the deadband, a small K_p should be used to reduce thruster activity. On the other hand when the input signal has a small amplitude and falls inside the deadband, a large K_p is required to force the input out of the deadband. In this case a large K_p can maintain linearity of the modulator and increase control accuracy. Using appropriate K_p according to the magnitude of input signals is an effective way to maintain modulator linearity and reduce thruster activity. In this paper a two-staged input gain K_p will be used, as to be discussed in a later section.

5. Minimum Pulse Width Determination

The effective deadband of the modular is defined as the minimum input to the modulator for which $T_{\text{on}} > 0$. Substituting Eq. (9) into Eq. (6) gives an expression for the minimum on-time, defined as the minimum pulse width. The minimum pulse width is usually dictated by relay operational constrains and is given by

$$T_{\min} = -\tau_m \ell_n[1 - h/(k_m U_m)] \tag{10}$$

B. PWPF Modulator Design Analysis

The objective of this analysis is to recommend appropriate PWPF modulator parameter settings for general use. The recommended settings will be used later for design of a PWPF modulator to modulate the command shaped by an input shaper. The design analysis is done by comparing performance indices for different modulator parameter settings with the help of MATLAB/Simulink.

1. *Static Analysis*

Simulations with a constant input $r = 0.5$ are performed to study the impact of parameters [$E_{\text{on}}\,(d)$, $E_{\text{off}}\,(d-h)$, k_m, and K_p] on the PWPF static performance indices: modulation factor, thruster firing frequency, thruster cycles, and total thruster on-time. Figure 3 plots the number of thruster firings vs E_{on} and $E_{\text{off}}/E_{\text{on}}$. This figure indicates that for $E_{\text{off}}/E_{\text{on}} > 0.8$ the thruster cycle increases much faster than it does for $E_{\text{off}}/E_{\text{on}} < 0.8$. Figure 3 shows that for $E_{\text{on}} < 0.2$ the thruster cycle increases much faster than it does for $E_{\text{on}} > 0.2$. To avoid excessive thruster firings, $E_{\text{on}} > 0.2$ and $E_{\text{off}}/E_{\text{on}} < 0.8$ are suggested in PWPF modulator designs. Simulations with varying k_m and K_p show that keeping $1 < k_m < 6.0$ and $2 < K_p < 10$ can maintain pseudolinear operation of a PWPF modulator without excessive thruster firings.[11] The preferred range of parameters is recommended in Table 2.

2. *Dynamic Analysis*

To study the impact of input frequency and the time constant on PWPF output phase lag and thruster activity, simulations are conducted by applying unity magnitude sinusoidal inputs to the PWPF modulator. Input frequencies are varied from 1 to 150 rad/s, and time constants are varied from 0.01 to 0.4s. Fixed modulator parameters are shown in Table 3 and are consistent with the recommendations in Table 2. The input gain is set to one.

Phase Lag. The result of the phase lag simulation is shown in Fig. 4. The value of phase lag, displayed on the vertical axis, is represented in terms of the percentage of a period of the input signal. For example, zero on the vertical scale indicates no phase lag. A value of 0.5 indicates a phase lag of 50% of an input period.

Note that for τ_m less than 0.2, there is little phase lag for all input frequencies. The plateau shown by a phase lag of 400% indicates the region of zero modulation factor. In this area the time constant is too large for the modulator to react to the high-frequency input. Note that for τ_m greater than approximately 0.2, the phase lag increases monotonically at low frequency. These characteristics suggest that τ_m should be kept less than 0.2 to reduce phase lag.

Thruster Activity. Figure 5 shows the effect of time constant and input frequency on thruster cycles. This graph suggests that a minimum time constant value of 0.1 should be maintained to avoid frequent thruster firings (Fig. 4). Further simulations also show that maintaining τ_m greater than 0.1 avoids excessive propellant use.

3. *Fourier Transform Analysis*

To better understand PWPF modulation, Fourier transform of the output of a PWPF modulator in pseudolinear operation is performed

Table 2 Static analysis results

Parameter	Recommended setting
Modulator gain, k_m	$1 < k_m < 6.0$
On-threshold, $E_{\text{on}}\,(d)$	>0.2
Off-threshold, $E_{\text{off}}\,(d-h)$	$<0.8d$
Input gain, K_p	$2 < K_p < 10$

Table 3 PWPF parameters in dynamic simulation

Parameter	Simulation value
K_m	4.5
$E_{\text{on}}\,(d)$	0.45
$E_{\text{off}}\,(d-h)$	0.15
U_m	1.0

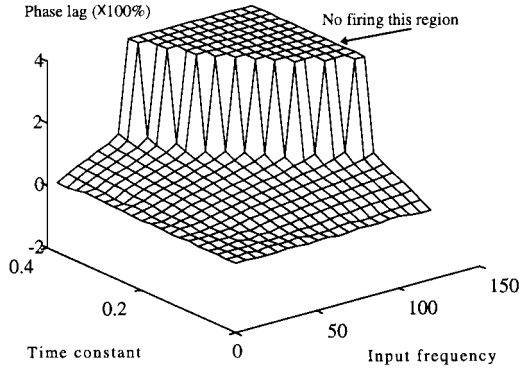

Fig. 4 Phase lag of PWPF output.

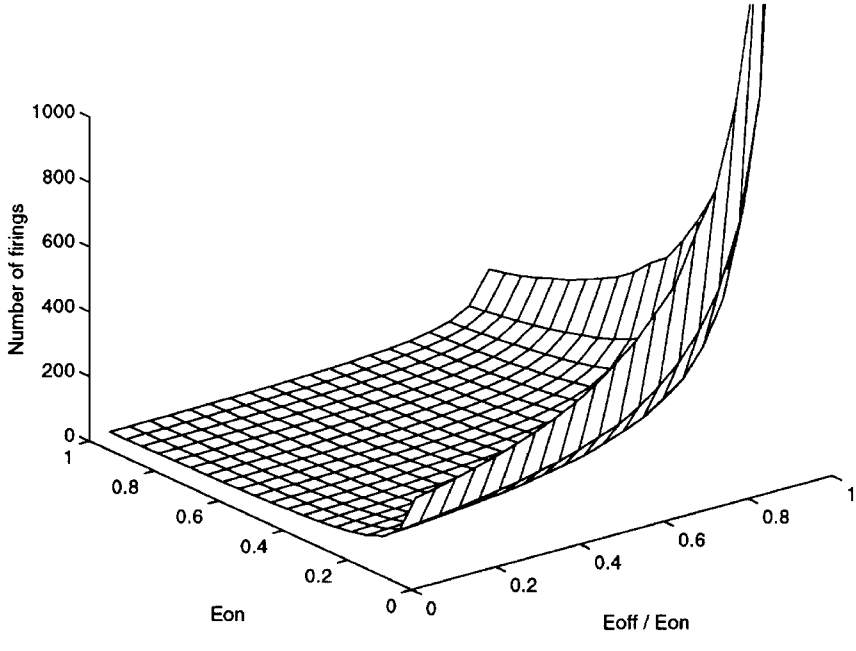

Fig. 3 Number of firings.

and compared with that of the input sinusoidal signal, as shown in Fig. 6. This figure indicates some minor frequency components in the PWPF output besides the main component (input frequency). These extra frequency components generated by a PWPF modulator must be taken into consideration when the modulator is used to modulate the command of an input shaper.

4. Design Recommendation

Table 4 summarizes the results from Secs. III.A and III.B and shows the recommended setting for each parameter. The PWPF parameter settings recommended in Table 4 can be used not only in this paper but also as general guidelines for PWPF modulator design.

Table 4 Summary of PWPF design analyses

Parameter	Static analysis	Dynamic analysis	Recommended settings
k_m	$1.0 < 6.0$	N/A	$1.0 < 6.0$
K_p	$2.0 < 10$	N/A	$2.0 < 10$
τ_m	N/A	0.1–0.2	0.1–0.2
$E_{\text{on}}(d)$	>0.3	N/A	>0.2
$E_{\text{off}}(d-h)$	$<0.8d$	N/A	$<0.8d$

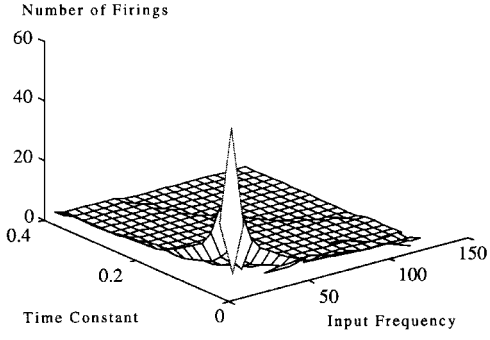

Fig. 5 Number of thruster cycles.

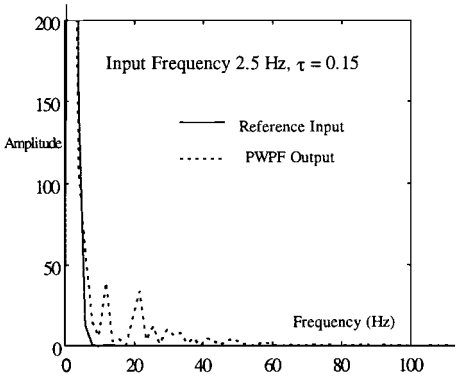

Fig. 6 Power spectral density plots.

IV. Command Input Shaping

Input shaping is the technique of convolving a sequence of impulses, an input shaper, with a desired command to a flexible structure so that the shaped command results in zero residual vibration. This technique is developed based on linear systems theory. A simple illustration of this technique is shown in Fig. 7. In this figure the vibration caused by the first impulse can be eliminated by applying an additional impulse of an appropriate amplitude and phase. This two-impulse train represents a zero vibration (ZV) shaper. The amplitude and timing of the impulse can be solved analytically for a linear system.

The ZV shaper offers the shortest pulse train that can cancel a single-mode vibration; however, it requires very good knowledge of the plant. Singer and Seering[12] showed that the ZV shaper was robust for only small variations ($\pm 5\%$) in modal frequency. To enhance a shaper's robustness, a zero vibration derivative (ZVD) shaper with three impulses and a zero vibration derivative derivative (ZVDD) shaper with four impulses were developed.[12] The ZVD shaper provides robustness for up to $\pm 20\%$ variations in frequency, and the ZVDD shaper allows plant uncertainties on the order of $\pm 40\%$ while retaining the ZV characteristics. Figure 8 illustrates the impulse train for a ZVDD shaper.

The pulse train parameters are given by

$$K = \exp\left(-\frac{\zeta\pi}{\sqrt{1-\zeta^2}}\right), \qquad \Delta T = \frac{\pi}{\omega_0\sqrt{1-\zeta^2}}$$

where ω_0 is the undamped modal frequency and ζ is the damping ratio for this the mode.

ZV, ZVD, and ZVDD shapers are designed for systems with proportional actuators, and they cannot be applied directly to systems with on-off actuators. By imposing constraints of constant-amplitude commands and maneuver requirements, ZV, ZVD, and ZVDD shapers are extended to constant amplitude pulse (CAP) shapers.[8,9] Obtaining a CAP shaper often involves complicated optimization. CAP shapers also result in bang-bang control action.

With the increase of the number of pulses used in the shaper, the shaped command will result in slower rigid-body response. Therefore, among ZV, ZVD, and ZVDD shapers, ZV has the fastest rigid-body response, and ZVDD has the slowest response.

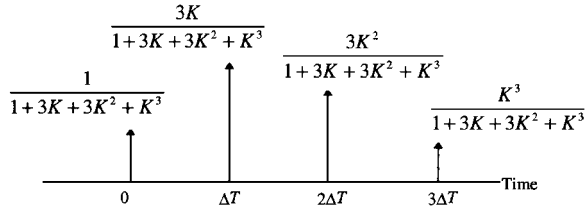

Fig. 8 Four-impulse ZVDD input shaper.

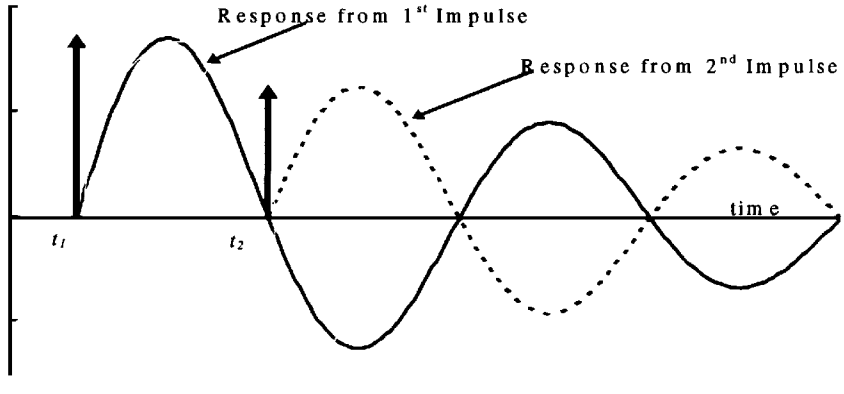

Fig. 7 Vibration cancellation using input shaping.

For multimode flexible systems the shaper aiming at one fundamental mode may excite a higher mode, but overall performance can be improved.

Compared with CAP shapers, variable-amplitudeshapers like ZV, ZVD, and ZVDD shapers have the advantage of simple computation because ZV, ZVD, and ZVDD shapers do not require optimization.

V. Integrated Input Shaper and PWPF Modulator for Vibration Reduction

A. PWPF Modulator

According to the recommended parameter settings in Table 4, the parameters of the PWPF modulator are chosen and listed in Table 5. This modulator will be used to modulate the commands that have been modified by an input shaper.

A two-staged design of K_p is intended to bring the PWPF modulator prefilter output above the deadzone level. When the input falls inside the deadzone, a large value of K_p is used; otherwise, the recommended minimum value is used.

The PWPF modulator parameter settings in Table 4 are general recommendations. The PWPF modulator parameters used in this case (shown in Table 5) can generally remain the same even when the modulator is used for a different shaper.

B. Input Shaper

As shown in Sec. III.B.3, the PWPF modulator does not exactly replicate the input command frequency. This motivates the use of a ZVDD shaper for increased robustness with respect to modal frequency. Because the goal is to suppress vibrations of low-frequency modes, a four-mode ZVDD shaper is chosen.

The design method presented in Sec. IV is used to generate the pulse trains for the ZVDD shaper. The resulting four-impulse sequence for each mode is given by

Table 5 PWPF parameters

Parameter	Value
K_m	1.25
K_p	2.0, input $> d/k_m$ 5.0, input $\leq d/k_m$
τ_m	0.15
$E_{\text{on}}\ (d)$	0.45
$E_{\text{off}}\ (d-h)$	0.15

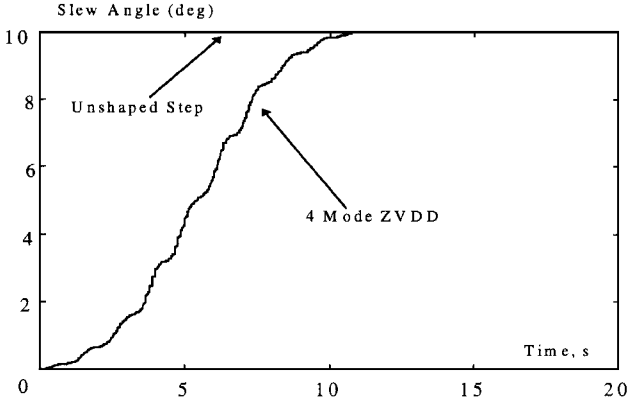

Fig. 9 Step command and the four-mode ZVDD command.

Mode i:

$$\begin{bmatrix} A_j \\ t_j \end{bmatrix} = \frac{1}{X_{DD}} \begin{bmatrix} 1 & 3K & 3K^2 & K^3 \\ 0 & \Delta T & 2\Delta T & 3\Delta T \end{bmatrix} \tag{11}$$

where K and ΔT are defined in Sec. IV and the sequence is unity normalized by

$$X_{DD} = 1 + 3K + 3K^2 + K^3$$

The resulting ZVDD pulse trains for modes 1–4 of the FSS are

Mode 1:

$$\begin{bmatrix} A_j \\ t_j \end{bmatrix} = \begin{bmatrix} 0.1274 & 0.3773 & 0.3726 & 0.1227 \\ 0 & 1.9563 & 3.9127 & 5.8690 \end{bmatrix}$$

Mode 2:

$$\begin{bmatrix} A_j \\ t_j \end{bmatrix} = \begin{bmatrix} 0.1274 & 0.3773 & 0.3726 & 0.1227 \\ 0 & 0.8273 & 1.6547 & 2.8420 \end{bmatrix}$$

Mode 3:

$$\begin{bmatrix} A_j \\ t_j \end{bmatrix} = \begin{bmatrix} 0.1274 & 0.3773 & 0.3726 & 0.1227 \\ 0 & 0.1719 & 0.3437 & 0.5156 \end{bmatrix}$$

Mode 4:

$$\begin{bmatrix} A_j \\ t_j \end{bmatrix} = \begin{bmatrix} 0.1274 & 0.3773 & 0.3726 & 0.1227 \\ 0 & 0.0980 & 0.1960 & 0.2940 \end{bmatrix}$$

Note that the amplitudes are the same due to the same damping assumed for all modes. The preceding four impulse trains are convolved to generate the four-mode ZVDD input as shown in Fig. 9. For comparison purposes the unshaped step command is presented in Fig. 9 as well. Using the shaped command, a longer settling time for the rigid-body is expected.

C. Vibration Reduction Using PWPF Modulated Input Shaper

The PWPF modulator proposed in Sec. V.A is used to modulate the four-mode ZVDD shaped command proposed in Sec. V.B. The primary goal is to reduce the lower-mode vibration of the FSS during a slew. As associated with an input shaper, worse performance in higher modes may be expected but should be in a limited range. Simulations are done to analyze the impact of the control with a PWPF modulated input shaper on rigid-body performance and flexible mode responses. The block diagram illustrating the FSS control system is shown in Fig. 10.

Figure 11 shows the lower-mode excitations resulting from a 10-deg slew maneuver. With all modal damping ratios of 0.004, the lower-mode flexible response is essentially undamped for the duration of the simulation when an unshaped step command is used. Using a four-mode ZVDD shaper with the PWPF modulator results in excellent cancellation of the targeted modes. Reductions in modal excitations of up to 95% are achieved in the first two modes

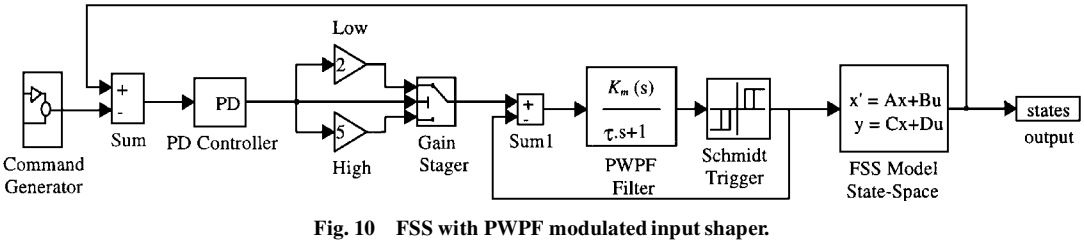

Fig. 10 FSS with PWPF modulated input shaper.

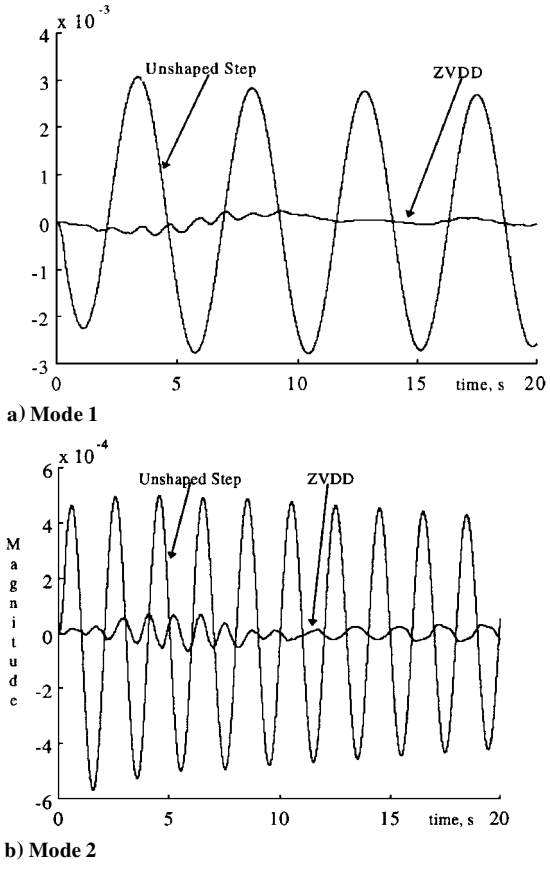

Fig. 11 FSS slewing with PWPF modulated ZVDD shaper.

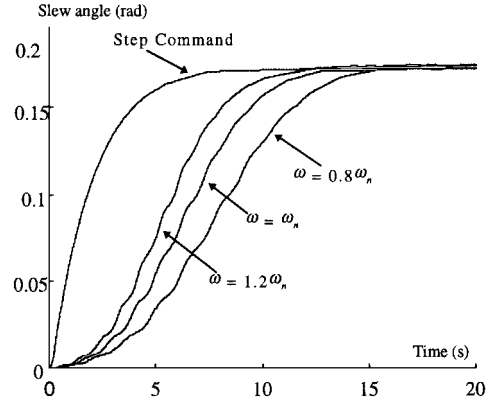

Fig. 12 Rigid-body response with ± 20% modal frequency uncertainty.

(Figs. 11a and 11b) and approximately 50% in the third mode. Vibration of mode 4 remains at about the same level.

Increased vibrations are found in modes 5 and higher. Worse performance in higher modes can be considered as the cost to achieve vibration reduction in lower modes. The increased vibration in higher modes is consistent with other research.[8] However, in this research, higher modes of excitation caused by a shaper designed a lower mode that is very limited. Therefore, it can be concluded that vibration reduction using an input shaper and a PWPF modulator is effective for flexible spacecraft with on-off actuators.

If lower modes must be completely eliminated, the multiple-mode shaper (like the four-mode ZVDD shaper proposed here) does the job at the cost of excitation of higher-frequency modes. On the other hand, if excitation of higher modes must be avoided and lower-mode vibration should be reduced but not eliminated, a single-mode or two-mode ZVDD shaper can be used.

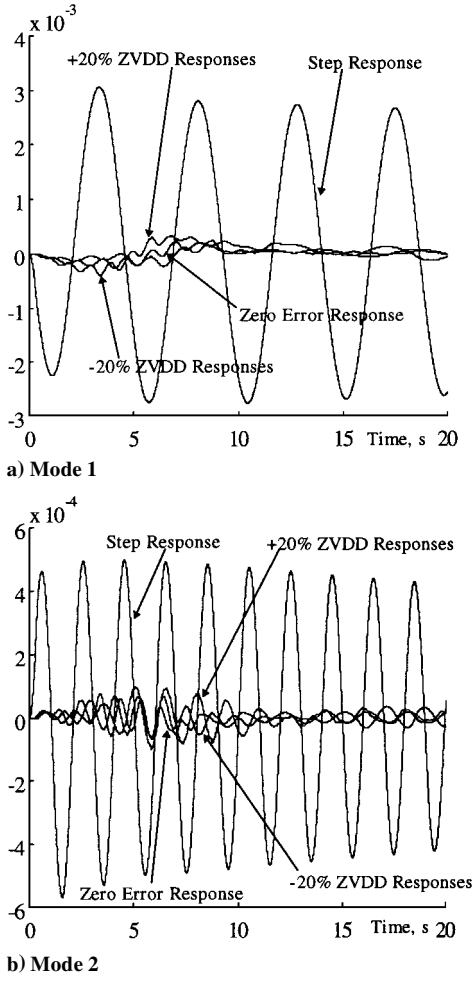

Fig. 13 ZVDD shaper robustness to 20% modal frequency uncertainty.

D. Robustness Analysis

Consider that in practice modal frequency generally can be obtained within ±20% error. The first simulation is run with ±20% errors in all four modal frequencies of the four-mode ZVDD shaper, and the results are compared with that of the case with exactly known modal frequencies. The rigid-body responses are shown in Fig. 12, and the first two mode responses are shown in Fig. 13. Figure 12 reveals that error in modal frequency slightly changes the settling time; however, it has little impact on the final stage error. Figure 13a shows that the case of −20% frequency error is very close to the nominal case, whereas the case of +20% frequency has a slightly increased vibration. Either case is robust with the error in modal frequency. Figure 13b also illustrates that ±20% frequency variations in all four modes have very limited influence on mode 2 vibration. Modes 3 and 4 show the same trend (figures not shown because of space limitation).

To further study the robustness, simulations are run using frequencies varying from $0.2\omega_n$ to $2.0\omega_n$ and damping ratios varying from 0.1ζ to 2.0ζ for all four modes of the four-mode ZVDD shaper. Flexible mode responses in terms of their average absolute displacement are shown in Figs. 14a–14d. Several observations are made here. First, vibration increases caused by ±20% modal frequency error are small for the first four modes (Figs. 14a–14d). Second, Fig. 14 reveals that the ZVDD shaper is almost insensitive to variations in damping. Third, the PWPF modulated shaper achieves well-behaved modal responses even for modal frequency errors of 100%.

The preceding three observations verify the robustness of the proposed vibration reduction method. In summary, integrating the techniques of command input shaping and PWPF modulation combines the advantages of variable amplitude input shapers and PWPF modulators. It provides a simple, effective, and robust method to suppress vibration on flexible spacecraft.

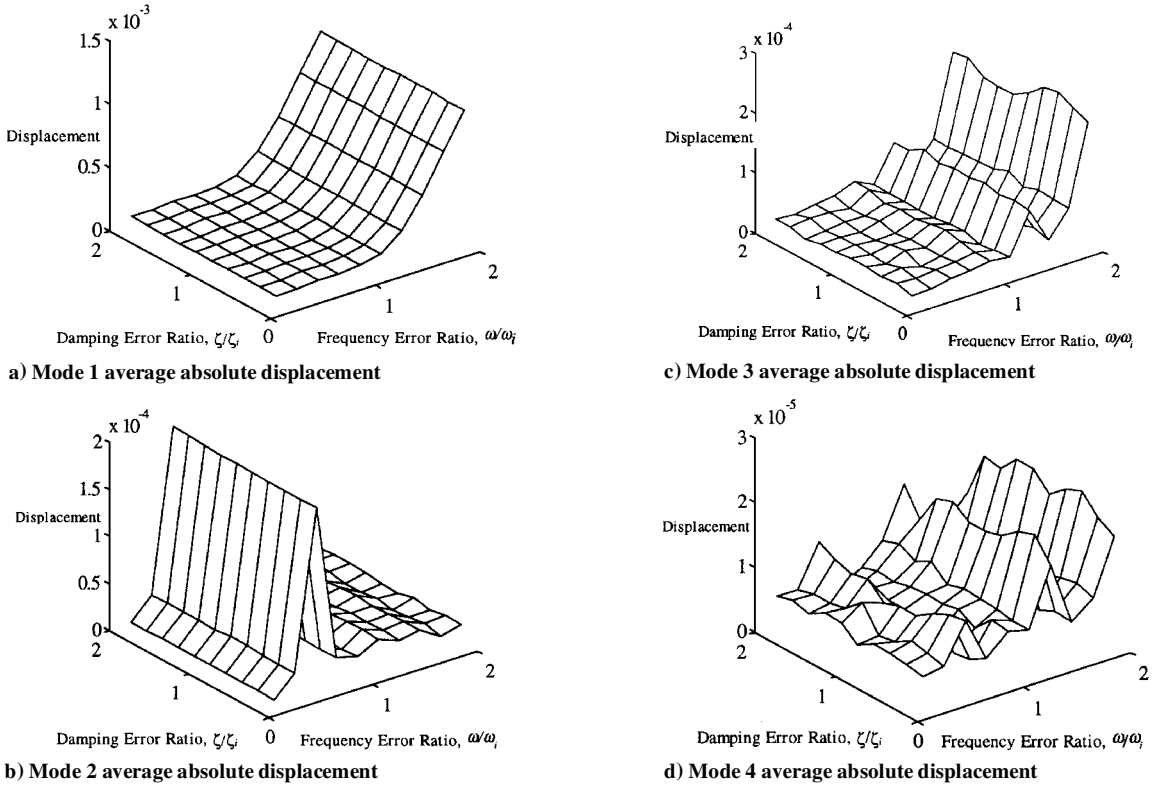

a) Mode 1 average absolute displacement

c) Mode 3 average absolute displacement

b) Mode 2 average absolute displacement

d) Mode 4 average absolute displacement

Fig. 14 Four-mode ZVDD shaper with modal frequency uncertainty and damping uncertainty.

VI. Conclusion

This paper presents the first study of a PWPF modulated thruster control using the technique of input shaping. The control object is the FSS at the U.S. Naval Postgraduate School. An analytical model of the FSS is developed to identify system frequencies. A detailed analysis of the PWPF modulator is performed to study the impact of modulator parameters on its performance. The PWPF modulator analyses reveal a narrow but effective tuning range for some modulator parameters. Subsequent investigations using a two-stage input gain validate the effectiveness of this technique. Use of the recommended design parameter ranges avoids excessive phase lag, minimizes thruster cycles, and keeps propellant use to a minimum. A command input shaper is designed and integrated with the PWPF modulator. Robustness analyses are performed to show the insensitivity of PWPF modulated input shapers to frequency and damping uncertainty. Numerical simulations performed on an eight-mode model of the FSS demonstrate the efficacy of the variable-amplitude shaped command with PWPF modulation.

Acknowledgments

The authors would like to express their gratitude to Y. Wang for his useful suggestions and to the anonymous reviewers for their helpful comments.

References

[1]Millar, A., and Vigneron, F. R., "Attitude Stability of Flexible Spacecraft Which Use Dual Time Constant Feedback Lag Network Pseudorate Control," AIAA Paper 76-266, April 1976.

[2]Clark, R. N., and Franklin, G. F., "Limit Cycle Oscillations in Pulse Modulated Systems," *Journal of Spacecraft and Rockets*, Vol. 6, No. 7, 1969, pp. 799–804.

[3]Hablani, H. B., "Multiaxis Tracking and Attitude Control of Flexible Spacecraft with Reaction Jets," *Journal of Guidance, Control, and Dynamics*, Vol. 17, No. 4, 1994, pp. 831–839.

[4]Bittner, H., Fischer, H. D., and Surauer, M., "Design of Reaction Jet Attitude Control Systems for Flexible Spacecraft," *Proceedings of the IFAC Automatic Control in Space Conference* (Noordwijkerhout, The Netherlands), International Federation on Automatic Control, Laxemburg, Austria, 1982, pp. 373–398.

[5]Wie, B., and Plescia, C. T., "Attitude Stabilization of Flexible Spacecraft During Stationkeeping Maneuvers," *Journal of Guidance, Control, and Dynamics*, Vol. 7, No. 4, 1984, pp. 430–436.

[6]Anthony, T., Wei, B., and Carroll, S., "Pulse-Modulated Control Synthesis for a Flexible Spacecraft," *Journal of Guidance, Control, and Dynamics*, Vol. 13, No. 6, 1990, pp. 1014, 1015.

[7]Crain, E., Singhose, W. E., and Seering, W. P., "Derivation and Properties of Convolved and Simultaneous Two-Mode Input Shapers," *Proceedings of the 13th Triennial IFAC World Congress* (San Francisco, CA), Vol. O, International Federation on Automatic Control, Laxemburg, Austria, 1996, pp. 441–446.

[8]Pao, L., and Singhose, W., "A Comparison of Constant and Variable Amplitude Command Shaping Techniques for Vibration Reduction," *Proceedings of the 4th IEEE Conference on Control Applications* (Albany, NY), Inst. of Electrical and Electronics Engineers, Piscataway, New Jersey, 1995, pp. 1120–1125.

[9]Singhose, W., Pao, L., and Seering, W., "Time-Optimal Rest-to-Rest Slewing of Multi-Mode Flexible Spacecraft Using ZVD Robustness Constraints," AIAA Paper 96-3845, Aug. 1996.

[10]Likins, P. W., and Fleischer, G. E., "Results of Flexible Spacecraft Attitude Control Studies Utilizing Hybrid Coordinates," *Journal of Spacecraft and Rockets*, Vol. 8, No. 3, 1971, pp. 264–273.

[11]Buck, N. V., "Minimum Vibration Maneuvers Using Input Shaping and Pulse-Width Pulse-Frequency Modulated Thruster Control," M.S. Thesis, Dept. of Astronautical Engineering, U.S. Naval Postgraduate School, Monterey, CA, Dec. 1996.

[12]Singer, N., and Seering, W., "Preshaping Command Inputs to Reduce System Vibration," *Transactions of the ASME Journal of Dynamic Systems, Measurement and Control*, Vol. 112, March 1990, pp. 76–82.